MECHANISTIC MODEL FOR THE PREDICTION OF TOP-OF-THE-LINE CORROSION RISK

Frédéric Vitse, Srdjan Nesic
Corrosion in Multiphase Systems Center
Institute for Corrosion and Multiphase Technology
Ohio University, Athens, OH 45701, U.S.A

Yves Gunaltun, Dominique Larrey de Torreben, Pierre Duchet-Suchaux
Exploration and Production TotalFinaElf
92069 Paris La Defense.

ABSTRACT

A model is presented for the prediction of the corrosion rate by CO_2 under dewing conditions. A mechanistic approach is developed that takes into consideration the hydrodynamics, thermodynamics, heat and mass transfer, chemistry, and electrochemistry during the phenomenon of Top-Of-The Line corrosion. This model is validated by experimental data. It offers a better insight on the role played by primary parameters such as the temperature, the total pressure, the partial pressure of CO_2, the gas velocity, and the condensation rate.

INTRODUCTION

In the case where a pipeline cannot be protected from internal corrosion by the injection of inhibitors of corrosion, a reliable control device and some accurate predictive tools of the corrosion rate are required. In the specific case of Top-of-the-Line Corrosion (TLC), the stratified or stratified-wavy flow regime does not provide a good wettability by inhibitors[1] of the upper part of the internal pipewall.

Non-inhibited water is present at the top of the line due to the condensation of water vapor transported along the pipe with other gas. As important heat exchanges take place between the pipe and its surrounding, a certain amount of water will condense at the pipewall leading to a corrosive environment[2]. In order to qualitatively and quantitatively describe the phenomena of corrosion occurring at the top of the line, a deep insight on the combined effect of the chemistry, hydrodynamics, thermodynamics and heat and mass transfer in the condensed water is needed[3].

In this paper, the corrosion rate in the presence of carbon dioxide is experimentally studied along with the condensation rate of water in a horizontal pipeline in the presence of a non-condensable gas. Particular attention is given to the following parameters: temperature of the gas

bulk, temperature of the pipewall, total pressure in the system, partial pressure of carbon dioxide, gas velocity, and condensation rate.

A mechanistic model is developed that gives a better insight on the role played by the aforementioned parameters. The model is tuned on a large set of experimental data and offers a convenient predictive tool for the risk of TLC by CO_2. This model can directly be used to optimize the design of pipelines since it allows the determination of the level of thermal insulation required to avoid the condensing conditions leading to an unacceptable rate of corrosion.

EXPERIMENTAL SETUP AND MEASUREMENT TECHNIQUES

Experimental setup and procedure

In order to reproduce the conditions encountered in the field during the production of wet gas, a full-scale flow loop was built in our laboratories. The schematic of the loop is given in Figure 1. The experimental procedure is as follow: carbon dioxide is first injected in the flow loop up to a specific pressure. In a 1 m^3 stainless steel tank, water is then heated by electrical resistances up to the temperature of interest. The pump is then started and the mixture flows in the 4-inch stainless-steel loop until the thermodynamic equilibrium between the gas phase, the pipe, and the surrounding is reached. A countercurrent double-pipe heat exchanger is used to cool the gas mixture and control the condensation rate. The condensed water can be collected in a pressure vessel. This configuration allows sampling without disturbing the flow and the pressure in the loop.

The real-time measurement of the corrosion rate starts once the system is at equilibrium. Data acquisition devices are set to continuously measure the inlet and outlet temperature of the gas bulk, the wall temperature at the position where the corrosion probe is installed, the total pressure, the gas velocity, the temperature at the inlet and outlet of the cooling liquid, the cooling liquid flowrate, and the corrosion rate. Figure 2 shows the design of the heat exchanger, the insertion ports for the flush-mounted probes, and the position of the data acquisition for temperatures and flowrates.

Setup and data acquisition for corrosion measurement

During TLC, it is particularly important to know the local wall temperature on the inner pipewall in addition to the bulk gas temperature. There are two reasons for this:

- Because the fluid transported is gas, and because significant heat exchanges occur at the wall, an important temperature gradient can occur between the bulk phase and the wall. In such a case, the wall temperature is more adapted than the bulk temperature to predict the kinetics of the electrochemical reaction of corrosion.
- The condensation rate of water vapor is going to be dependent on the heat and mass transfer in the gas phase. These transfers are related to the gradient of temperature occurring between the gas bulk and the pipewall. Thus, an accurate measurement and control of the wall temperature is needed to set the local condensation rate.

For these reasons, the probe used for the measurement of the corrosion rate must be kept at the same temperature as the rest of the wall. A new technology of "air-cooled" corrosion probe is used and validated for this specific project. By allowing a flow of air through the body of the probe, the

temperature of the sensing element can be kept identical to the wall temperature. A data acquisition system linked to a thermosensor in the probe head allows such monitoring.

The new probe was designed to be either flush-mounted to the pipe or slightly retracted within the pipewall. This last configuration simulates a formed cavity in the pipewall, which is often the case during TLC. The geometry of the probe head and its positioning with respect to the pipewall is going to greatly influence the local hydrodynamics of the condensed water. In this sense, it is also expected to influence the corrosion rate.

The Electrical Resistance (ER) measurement technique is used during experimentation on TLC. Electrochemical techniques are avoided for several reasons: the conductivity of condensed water may be too low to give a reasonable reading. Also, at low condensation rates, the condensed water film on the probe head may not be continuous, preventing the current to flow between the working and the counter electrode. Some additional Coupon Weight Loss measurements (CWL) are run simultaneously to ER to validate the experimental results. For CWL measurements, the same type probe body (air cooled) is used.

EXPERIMENTAL RESULTS

In some cases, the effect of some primary parameters on the condensation rate and on the corrosion rate can be isolated by keeping the other parameters of experimentation as constants. In other cases, the parameters of interest are coupled and so is their effect on the corrosion and condensation rate. All the following tests were run over a period of time from 48 hours to 120 hours. For each test, the corrosion rate reported is the stabilized rate (the corrosion rate is considered stable when no change larger than 0.05 mm/y occurs during a period of time of at least 12 hours).

Influence of the bulk temperature and the wall temperature on the corrosion rate

The influence of temperature was studied over a range from 40°C to 100°C. First, as the temperature increases, the corrosion rate increases as well. The maximum corrosion rate is reported at 70°C. Then, the trend is reversed and the corrosion rate decreases as the temperature increases to 90°C. The condensation rate, however, keeps increasing as the temperature increases. As can be seen from Figure 3, the same trend with a maximum corrosion rate around 70 or 80°C is observed no matter what the CO_2 partial pressure of the system is.

These results can be interpreted as follows: at lower temperatures (below 70°C), the corrosion rate increases with temperature according to Arrhenius' law applied to the endothermic reaction of corrosion by CO_2. At higher temperatures (above 80°C), the corrosion rate decreases as temperature increases suggesting that an additional phenomenon occurs for such temperatures. There are at least three possible explanations for this. At higher temperatures, the condensation rate is more important and the condensed liquid film at the wall is thicker. Therefore, the mass transfer of corrosive species through the condensed liquid to the wall may be limiting, which may explain a lower corrosion rate. Another explanation is that, at higher temperature, the precipitation on the wall of the products of corrosion as an iron carbonate layer may partially protect the metal from further corrosion. The third explanation may be that at higher temperature, and thus, at higher corrosion rates, the amount of iron ions present in the condensed water is larger, which increases

the pH of the water. The change in pH may, in turn, change the mechanism of the electrochemical reaction at the wall[4]. Therefore, the corresponding corrosion rate may become smaller with time. These two last assumptions are in agreement with the experimental fact that the corrosion rate should be significantly smaller at low condensation rates, as is clearly observed in Figure 3. At a CO_2 partial pressure of 4 bar and a temperature of 70°C, the corrosion rate is found to be 4 times higher under intense dewing conditions than the rate obtained under low condensation.

Influence of the partial pressure of carbon dioxide on the corrosion rate

The influence of the partial pressure of carbon dioxide is studied over a range from 1 to 8 bars at a bulk temperature of 50, 70, and 90°C and at low and high condensation rates. The experimental results regarding the corrosion rate are plotted in Figure 4. It can be seen that the partial pressure has little influence on the corrosion rate, both at 50°C with cooling and at 90°C without cooling. On the other hand, at 70°C and at 90°C with high cooling, the influence of the partial pressure of carbon dioxide is more significant. As the partial pressure doubles, the corrosion rate increases 40% at 70°C and more than 110% at 90°C. Comparatively, de Waard's correlation[5] predicts a 60% increase as the partial pressure of carbon dioxide doubles. It appears from our experimental data that the corrosion rate is sensitive to a change in partial pressure of carbon dioxide at high condensation rates but is insensitive to such a change at low condensation rates. At low condensation rates, it may be easier to saturate, or even supersaturate, the condensed liquid with the products of corrosion, thus increasing the pH, and somehow, slowing down the kinetics of the reaction of corrosion by CO_2. At higher condensation rates, the buffering of the pH of the solution by iron ions may be insignificant and the pH might be more sensitive to the change in partial pressure of carbon dioxide.

Influence of the gas velocity on the corrosion rate

The influence of gas velocity on the corrosion was studied over a range from 2 to 8 m/s. It was studied both at 90 and 50°C. At high temperatures, the stabilized corrosion rate does not seem to be significantly affected by the change of gas velocity. On the other hand, a sudden change of the corrosion rate is observed at 50°C as the gas velocity drops from 4 to 2 m/s.

It appears that the gas velocity does not have a direct effect on the corrosion rate, but rather on the condensation rate, which, in turn, may affect the corrosion rate. This is clearly demonstrated by Figure 5 where both the condensation rate and the corrosion rate are reported as a function of the gas velocity: at 90°C as well as at 50°C, the condensation rate decreases significantly as the gas velocity varies from 8 to 2 m/s. Mass transfer in the gas phase is less important for a less turbulent flow (low velocities). Therefore, less water is available for condensation at the wall and less heat is removed, preventing the phase change of the water vapor. Meanwhile, the corrosion rate remains unaffected by a change of gas velocity, except when this change lowers the condensation rate below a critical value.

Influence of the condensation rate on the corrosion rate

From this experimental study, it appears that the condensation rate is dependent on all other primary parameters without exception. This complex dependence is discussed elsewhere[3]. This

renders the prediction of the condensation rate difficult. However, it appears from the previously reported experimental data that the role of the condensation rate is central in the determination of the corrosion rate during TLC. Therefore, its influence on the corrosion rate is studied at last. In the previous paragraph, it was reported that it is in the lower range of condensation rates that a significant influence on the corrosion rate can be observed. Thus, the influence of the condensation rate was studied at 50°C, where lower condensation rates were obtained with the experimental setup previously described. It was made possible to change the condensation rate of an order of magnitude, only by changing the temperature of the pipewall by a few degrees. Results show that the corrosion rate significantly increases as the condensation rate crosses a threshold. Below this threshold, the corrosion rate measured with respect to time by the ER probe initially sharply decreases and later stabilizes at a comparatively lower value (see Figure 6). Above the threshold, the corrosion rate remains constant in time, even in the first hours of experimentation and at a comparatively higher value. The concept of a critical threshold for the condensation rate is in agreement with the theory of a corrosion rate controlled by the level of supersaturation of the condensed water by the products of corrosion. At high condensation rates, the bulk of the condensed water may never get saturated. In this case, the corrosion rate would not significantly be dependent on the condensation rate, since no significant increase of the iron ion concentration is possible, and therefore, no significant change in pH can occur. At low condensation rates, the water is more likely to become supersaturated with the products of corrosion. In this case, the corrosion rate would be affected by a higher pH and a lower availability of corrosive species in solution. If the temperature is high enough, the formation of a scale of iron carbonate may be possible, which could further decrease the corrosion rate. In-between these two regimes of corrosion, a transition regime may exist, where the pH of condensed water changes rapidly with small perturbations of the primary parameters. Therefore, the sensitivity of the corrosion rate to the condensation rate, the wall temperature, and the partial pressure of carbon dioxide would be greater. This theory may explain the sudden jumps in the corrosion rate observed during a slight change of the condensation rate around the critical threshold.

MODELING OF THE CORROSION RATE

In order to predict the corrosion rate during TLC as a function of the internal parameters and the heat exchanges with the surrounding, a better insight into the fundamental phenomena involved during corrosion under condensing conditions is needed. In particular, the condensation rate needs to be predicted before any prediction can be made of the corrosion rate.

Modeling the condensation rate of water vapor in horizontal pipelines in the presence of carbon dioxide

The heat and mass transfer between the gas bulk and the wall can be modeled by an equivalent circuit of heat and mass transfer resistances as shown in Figure 7. Each of these resistances must be determined to obtain the condensation rate at the wall:
- The heat and mass transfer resistances in the gas phase are obtained from the Dittus and Boetler's correlation for full pipe flow[6] adapted to the special case of low condensation at the wall[7].

- The heat and mass transfer resistances in the condensed liquid derive from Nusselt's theory[8]. adapted to the cylindrical geometry of a pipe[2].
- The heat transfer resistance of the pipewall and its coating are usually known from the suppliers.
- The correlation giving the external heat transfer resistance for the specific case of a double-pipe countercurrent heat exchanger is found in the literature[6,9]. In the field case, the external conditions surrounding the pipeline may vary greatly from one line to another and so do the corresponding external heat transfer resistances.

This model has proven its ability to predict accurately the condensation rate of water vapor in horizontal pipelines in presence of carbon dioxide[3]. The model takes into consideration the influence of the bulk temperature, the total and partial pressure, the cooling rate and the gas velocity.

Modeling the corrosion rate during TLC

During this study, the influence of 3 main phenomena occurring during TLC was modeled and the results of simulation were tested against experimental data:
- The influence of mass transfer of corrosive species through the condensed liquid film to the wall.
- The change of chemistry in the condensed liquid at the top of the line and the corresponding change in pH
- The influence of the formation of a corrosion product layer on the wall

Influence of the mass transfer in the condensed liquid

For this specific study, a two-dimensional, transient, Computational Fluid Dynamic code was developed[3] solving the mass transfer of corrosive species in the condensed liquid film with the following boundary conditions:
- Vapor-liquid thermodynamic equilibrium at the gas-condensed liquid interface
- Flux of consumption of species at the wall according to the kinetics of the electrochemical reaction involved. The corrosion rate can be obtained either from the semi-empirical model developed by de Waard[5] or by the mechanistic model developed by Nesic[4] .

Both convective and diffusive fluxes in the condensed liquid are solved and the temperature profile in the thin film is assumed to be linear. Results show that the corrosion rate obtained at steady state is dependent on the thickness of the condensed liquid film (see Figure 8). However, this model fails in predicting the experimental results showing a decrease of the corrosion rate as the condensation rate decreases; the phenomena of a film deposition and an increase of the pH due to the accumulation of the products of corrosion in the condensed water were not taken into consideration during this simulation.

Influence of the change in chemistry of the condensed water

During the reaction of corrosion, iron ions are produced and released into the condensed water. If the saturation of the water is reached, these iron ions combine with carbonate ion to form iron carbonate:

$$Fe^{2+} + CO_3^{2-} \rightarrow FeCO_3$$
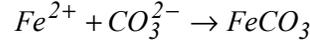
Iron carbonate is a solid that deposits on the surface of the pipe. Under certain conditions to be determined, the deposited layer can protect the metallic wall from further corrosion. Figure 9 represents a control volume of condensed water attached to the pipewall. The transport, source and sink of iron ions in this condensed water are also pictured. A material balance applied to the condensed water gives:

$$\frac{d(V \times [Fe^{2+}])}{dt} = \Phi_c \times A_c - \Phi_p \times A_p - \dot{m} \times A_{cond} \times [Fe^{2+}] \qquad (1)$$

V is the volume of condensed water (m^3), $[Fe^{2+}]$ is the concentration of iron ions in solution (kmol/m^3), Φ_c is the corrosion rate (kmol/m^2/s), A_c is the area where corrosion takes place (m^2), Φ_p is the precipitation rate (kmol/m^2/s), A_p is the area where precipitation takes place (m^2), $\dot{m}$ is the condensation rate (m^3/m^2/s), and A_{cond} is the area where condensation takes place (m^2). If one assumes that the area of corrosion, precipitation and condensation are equal and if it is further assumed that the condensed film thickness δ is known, Equation 1 becomes:

$$\frac{d([Fe^{2+}])}{dt} = \frac{1}{\delta} \times \left[\Phi_c - \Phi_p - \dot{m} \times [Fe^{2+}] \right] \qquad (2)$$

In absence of the formation of a protective scale, the corrosion rate Φ_c is determined according to the electrochemical model developed by Nesic[4]. According to this model, the computation of the corrosion rate requires knowledge of the concentration of dissolved carbon dioxide, of carbonic acid, and of protons. These concentrations can be obtained, once the iron concentration is known, by solving the equations of the thermodynamic equilibrium between the gas phase and the liquid phase, the equation of dissolution of carbon dioxide, the equation of electroneutrality, and the equations of dissociation of carbonic acid:

$$CO_{2(g)} \Leftrightarrow CO_{2(l)} \qquad (3)$$

$$CO_{2(l)} + H_2O \Leftrightarrow H_2CO_3 \qquad (4)$$

$$H_2CO_3 \Leftrightarrow H^+ + HCO_3^- \qquad (5)$$

$$HCO_3^- \Leftrightarrow H^+ + CO_3^{2-} \qquad (6)$$

$$\sum_{i=1}^{N} z_i c_i \qquad (7)$$

The value of the equilibrium constants corresponding to these reactions are given elsewhere[4].

The condensation rate is determined according to the theory of filmwise condensation presented earlier. The work done by Van Hunnik[10] can be used here to determine the precipitation rate. Under the assumption that, at the top of the line, the surface tension force determines the hydrodynamics of the film, the film thickness δ is obtained from the work of Gerstmann[11]. The author reports an average film thickness on the underside surface of a horizontal plate to be:

$$\delta = \left(\frac{\sigma}{g \times (\rho_l - \rho_g)} \right)^{1/2} \qquad (8)$$

σ is the surface tension coefficient, g is the gravity constant, ρ_l is the liquid density and ρ_g is the gas density. Equation 2 can be discretized in time as follow:

$$[Fe^{2+}]_{t+dt} = [Fe^{2+}]_t + \frac{\Delta t}{\delta} \times \left[\Phi_c(t) - \Phi_p(t) - \dot{m} \times [Fe^{2+}]_t \right] \qquad (9)$$

The computational procedure gives the change in pH as the iron concentration increases according to Equation 9. The corresponding corrosion rate is calculated and allows the prediction of the new concentration of iron ion at the next time step. The iteration continues until no further change in the iron ion concentration is computed.

Experimental and theoretical corrosion rates, as well as the corrosion rate according to de Waard's model (presently modified to take into consideration the mass transfer in the condensed film as described previously), are also plotted against the temperature, the partial pressure, and the condensation rate in Figures 10, 11, and 12, respectively. In general, the corrosion rate is overpredicted by both of the models. Moreover, the present model shows an increase in the corrosion rate as the temperature increases above 80°C whereas the experimental corrosion rate decreases above such temperature. The overprediction of the corrosion rate is due to the fact that further protection of the depositing iron carbonate scale on the metal is not taken into consideration. According to the present model, the influence of the temperature on the corrosion rate at low condensation rate is predominant: experimentally, as the normalized condensation rate* increases from 0.02 to 0.03, the corresponding wall temperature decreases from 52°C to 48°C. Accordingly, the predicted normalized corrosion rate* decreases from 1.42 to 1.26. Experimentally, an increase in the corrosion rate from 0.14 to 0.32 was observed, suggesting that at low condensation rates, the influence of the condensation rate on the corrosion rate is predominant rather than the influence of temperature. It appears that the sensitivity of the model to the change in condensation rate is not sufficient. Clearly, neither the influence of the

hydrodynamics, nor the influence of the chemistry of the condensed water is sufficient to predict the corrosion rate during TLC. Even if the prediction of corrosion rate is less conservative when the saturation of the condensed water by products of corrosion is taken into consideration, the theoretical results still overpredict the experimental ones by one order of magnitude. Therefore, the formation of a scale that deposits on the metal surface and partially protects it from further corrosion is necessary. An approach for the modeling of the influence of an iron carbonate scale on the corrosion rate is developed in what follows.

Influence of the deposition of an iron carbonate scale

The role of a protective scale can be grossly simplified by considering that part of the corroding surface is now covered by the products of corrosion and, on a covered site, no further corrosion occurs. On the uncovered surface, only corrosion occurs. If one considers that the scale covers a percentage (1-K) of the corroding surface, K being greater than or equal to 0 and smaller than or equal to 1, the material balance presented in Equation 2 becomes:

$$\frac{d([Fe^{2+}])}{dt} = \frac{1}{\delta} \times \left[K \times \Phi_c - (1-K) \times \Phi_p - \dot{m} \times [Fe^{2+}] \right] \tag{10}$$

The discretized form of this equation is:

$$[Fe^{2+}]_{t+dt} = [Fe^{2+}]_t + \frac{\Delta t}{\delta} \times \left[K \times \Phi_c(t) - (1-K) \times \Phi_p(t) - \dot{m} \times [Fe^{2+}]_t \right] \tag{11}$$

Following the same computational procedure as the one developed for the prediction of the corrosion rate in absence of a protective scale but using Equation 11 rather than Equation 9, the chemistry of the water during scaling conditions can be derived in time. The iterative computation of the iron ion concentration converges to give the corrosion rate at steady state in presence of a protective scale.

The surface coverage (1-K) is determined by tuning the mechanistic model developed here so that it fits the experimental corrosion rates obtained from 17 experiments run over a wide range of temperatures, partial pressures of carbon dioxide, and condensation rates. K is plotted as a function of the scaling tendency[12] in Figure 13. The scaling tendency is defined as the ratio of the precipitation rate (in $kmol/m^2/s$) to the corrosion rate in absence of a scale (in $kmol/m^2/s$). From Figure 13, it can be seen that the results are distributed in a stepwise manner. Below a scaling tendency of 0.7, K remains almost constant and within a range from 0.2 to 0.3. Above a scaling tendency of 0.7 and up to 0.99, K drops to a stable value around 0.1. Above a scaling tendency of 0.99, K decreases quickly to values as low as 0.01.

$$* \ Normalized \ corrosion \ rate = \frac{corrosion \ rate}{maximum \ experimental \ corrosion \ rate}$$

$$* \ Normalized \ condensation \ rate = \frac{condensation \ rate}{maximum \ experimental \ condensation \ rate}$$

The observed results are in agreement with the ones published by Pots[12] in the sense that the protectiveness of a scale seems to correlate well with the scaling tendency. Pots reports a critical scaling tendency of 0.5 for a scale to become protective. In the case of TLC, the protectiveness of the scale is related in a stepwise manner to the scaling tendency, corresponding to different "levels of coverage" of the surface. For a scaling tendency close to one, the coverage is almost total. For a scaling tendency below 0.7, the coverage is around 70% of the corroding surface.

CONCLUSIONS

A model has been developed that gives a better insight into the mechanisms involved during TLC. In particular, the influence of the mass transfer in the condensed liquid film, of the saturation of the condensed liquid with the products of corrosion, and of the formation of an iron carbonate scale, have been studied. A full-scale flow-loop for TLC experimentation has been designed at the Institute for Corrosion and Multiphase Technology and a new generation of corrosion probes has been selected and validated to obtain experimental corrosion rates during TLC. Even if they play a role in the determination of the corrosion rate, neither the mass transfer nor the chemistry of the condensed water can completely explain the experimental data obtained at the Institute for Corrosion and Multiphase Technology. By introducing the surface coverage to take into consideration the influence of a deposited iron carbonate scale, it is possible to tune the mechanistic model with the experimental data. The surface coverage can then be correlated with the scaling tendency. The surface coverage is found to correlate in a stepwise manner with the scaling tendency.

REFERENCES

1. Estavoyer M., "Corrosion problems at Lack sour gas field", NACE publication "H2S corrosion in oil and gas production", page 905, Houston Texas, 1981.

2. Vitse F., Alam K., Gunaltun Y., Larrey de Torreben D., Duchet-Suchaux P., "Semi-empirical model for prediction of the Top-Of-the-Line corrosion risk", Corrosion/2002, paper no. 2245 (NACE International 2002).

3. Vitse F., "Experimental and theoretical study of the phenomena of corrosion by carbon dioxide under dewing conditions at the top of a horizontal pipeline in presence of a non-condensable gas", PhD dissertation, Ohio University, November 2002.

4. Nesic S., Postlethwaite J., Olsen "An electrochemical model for prediction of CO2 corrosion", Corrosion/1995, paper no. 131, (NACE International, 1995).

5. De Waard C., Lotz U., "Prediction of CO2 corrosion of carbon steel", Corrosion/1993, paper no. 69, (NACE International, 1993).

6. Dittus, F. W., L.M.K. Boetler: Univ. Calif. (Berkeley) Pub. Eng., vol. 2, p443, 1930.

7. Stephan, K. and Laesecke, A.: "The influence of suction on the heat and mass transfer in condensation of mixed vapors" . Warme Stoffubertrag. Vol 13 (1980) pp 115-123.

8. Nusselt, W.: Die Oberflachenkondensation des Wasserdampfes. VDI Z. 60(1916), pp 441-546, 569-575.

9. Chen X., Hawkins P., and Solberg D.: Trans. Am. Soc. Eng., vol. 68, 1946, p99.

10. Van Hunnik, E. W. J., "The formation of protective FeCO3 corrosion product layers in CO2 corrosion, Corrosion/1996, paper no6, (NACE International 1996).

11. Gerstmann J., Griffith P, "Laminar film condensation on the underside of horizontal and inclined surfaces". Int. J. Heat Mass Transfer, Vol 10, pp 567-580, 1967

12. Pots B. F. M. and Hendriksen E. L. J. A, "CO2 corrosion under scaling conditions - the special case of top-of-line corrosion in wet gas pipelines", Corrosion/2000, paper no. 31.
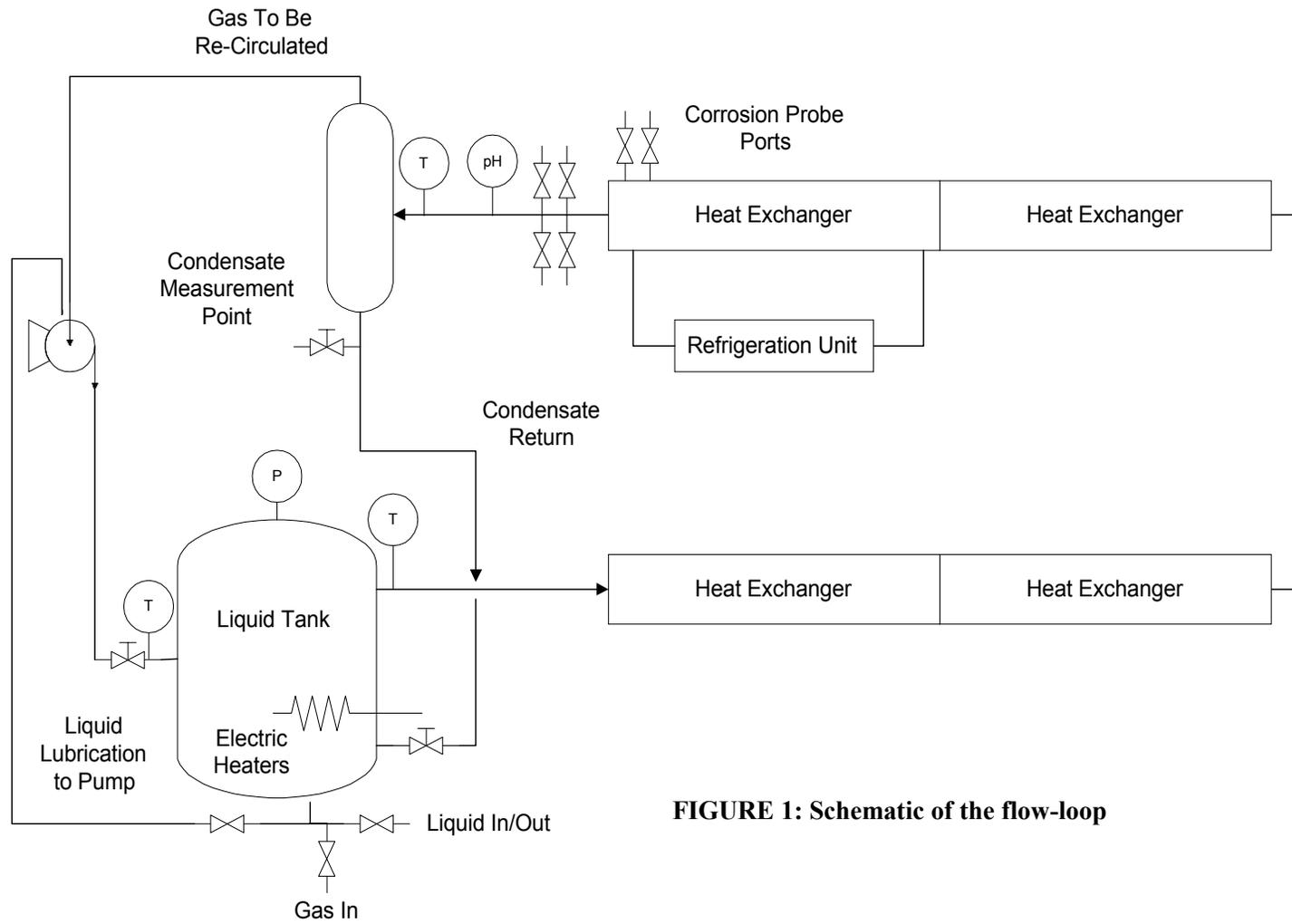
FIGURE 1: Schematic of the flow-loop
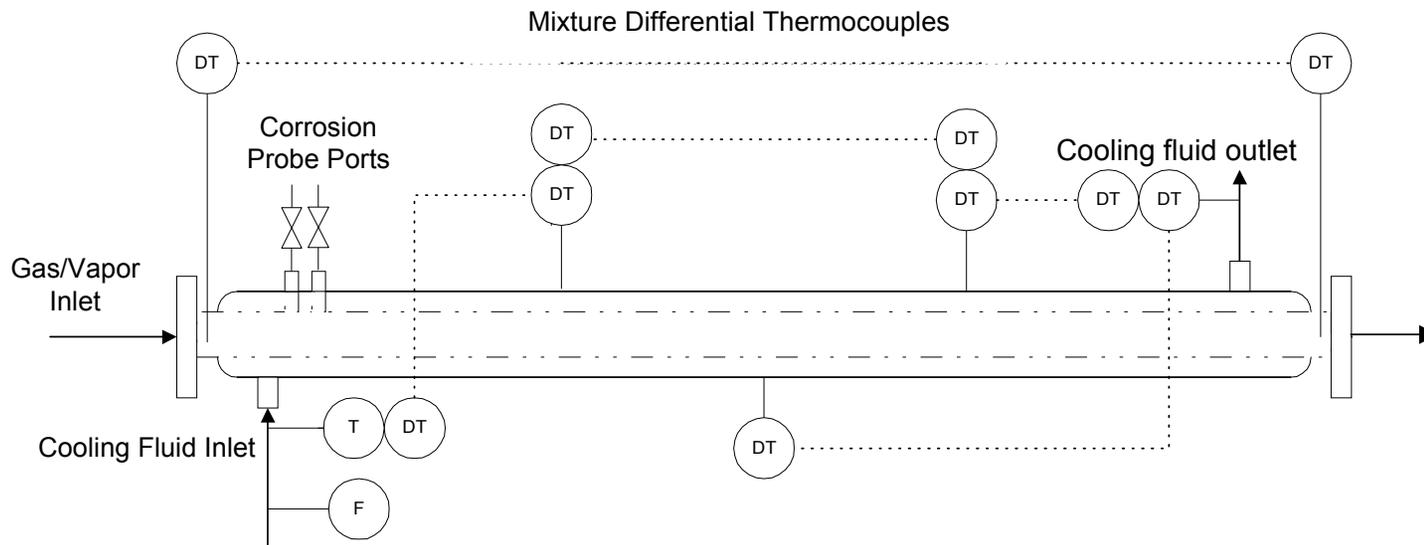
FIGURE 2: Double-pipe counter-current heat exchanger design

Notations:

In what follows:

*Normalized corrosion rate = $\dfrac{\text{corrosion rate}}{\text{maximum experimental corrosion rate}}$

*Normalized condensation rate = $\dfrac{\text{condensation rate}}{\text{maximum experimental condensation rate}}$
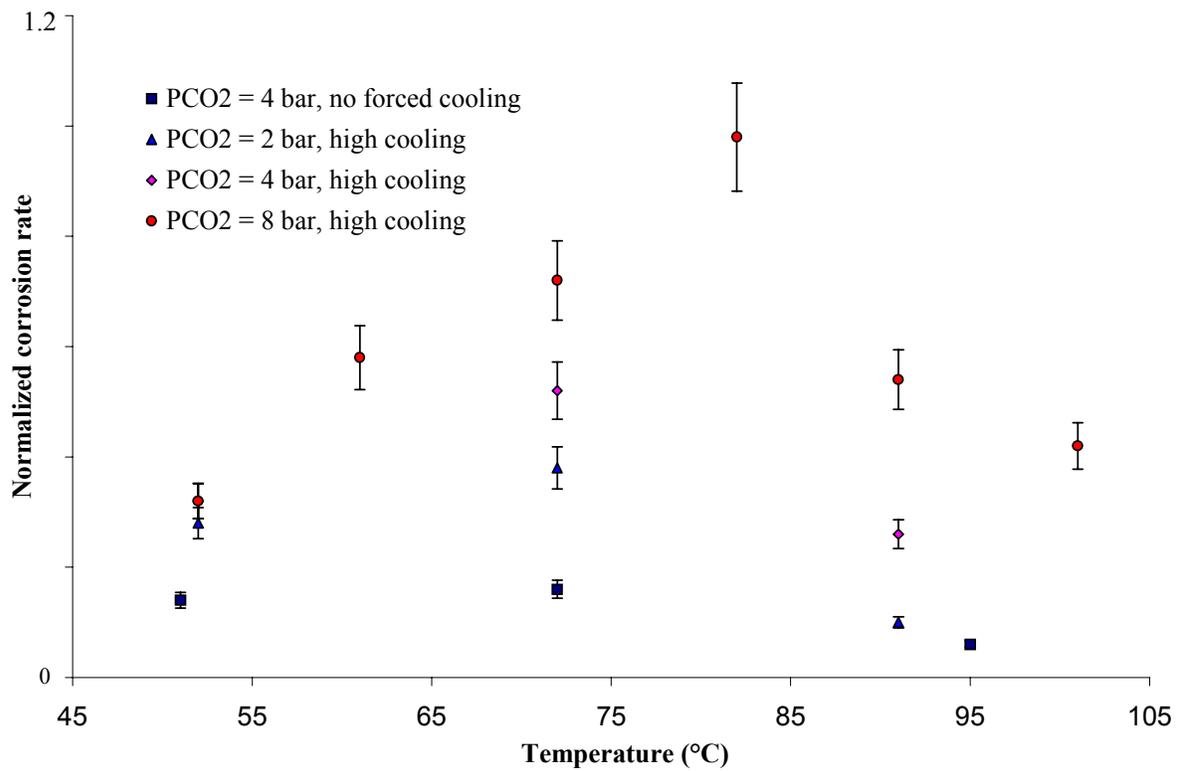
**FIGURE 3: Influence of gas temperature on the corrosion rate
at different partial pressures of CO_2 and different cooling rates.V_{gas} = 8m/s**
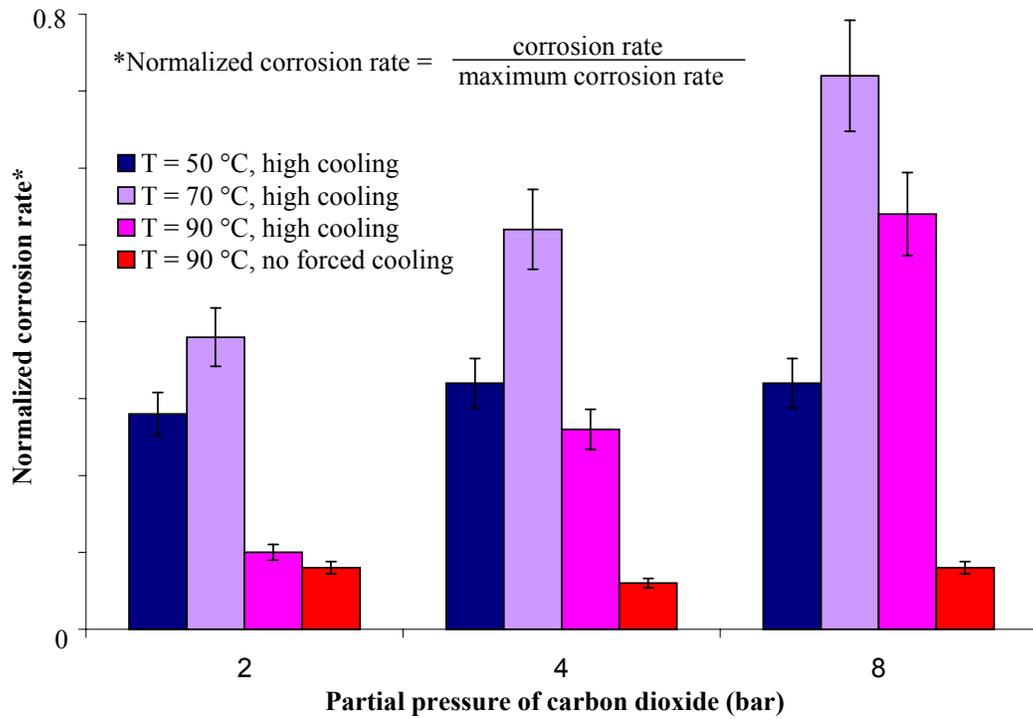
FIGURE 4: Influence of the partial pressure of carbon dioxide on the corrosion rate. V_{gas} = 8m/s.
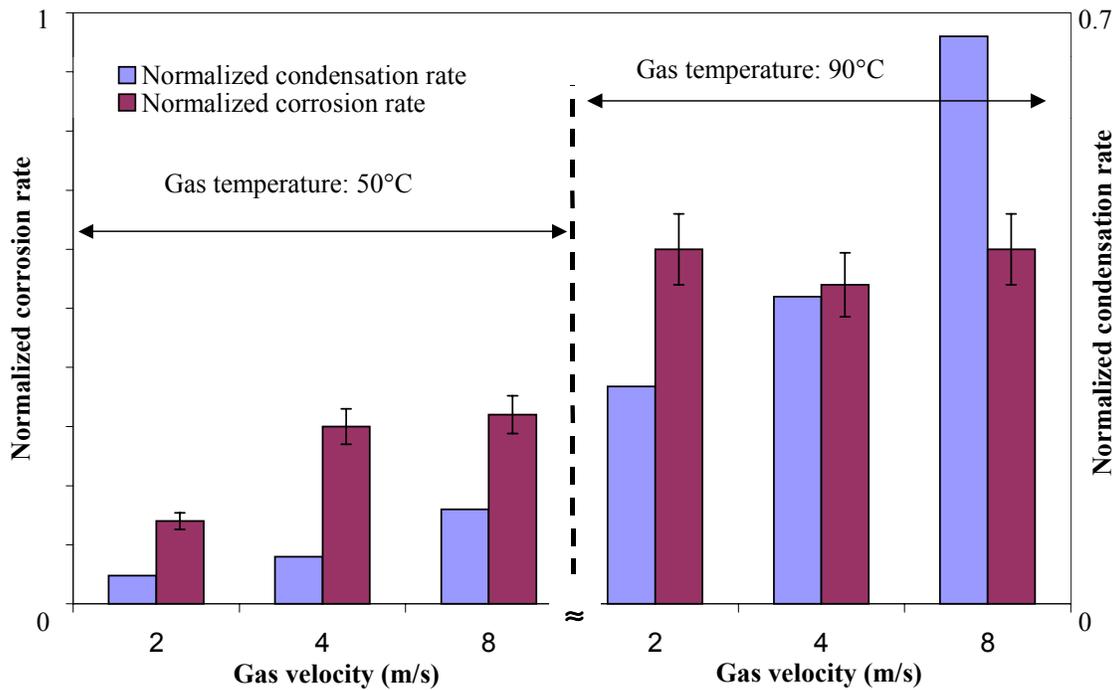
**FIGURE 5: Influence of the gas velocity on the condensation rate
and on the corrosion rate. High cooling, P_{CO2} = 8 bar**
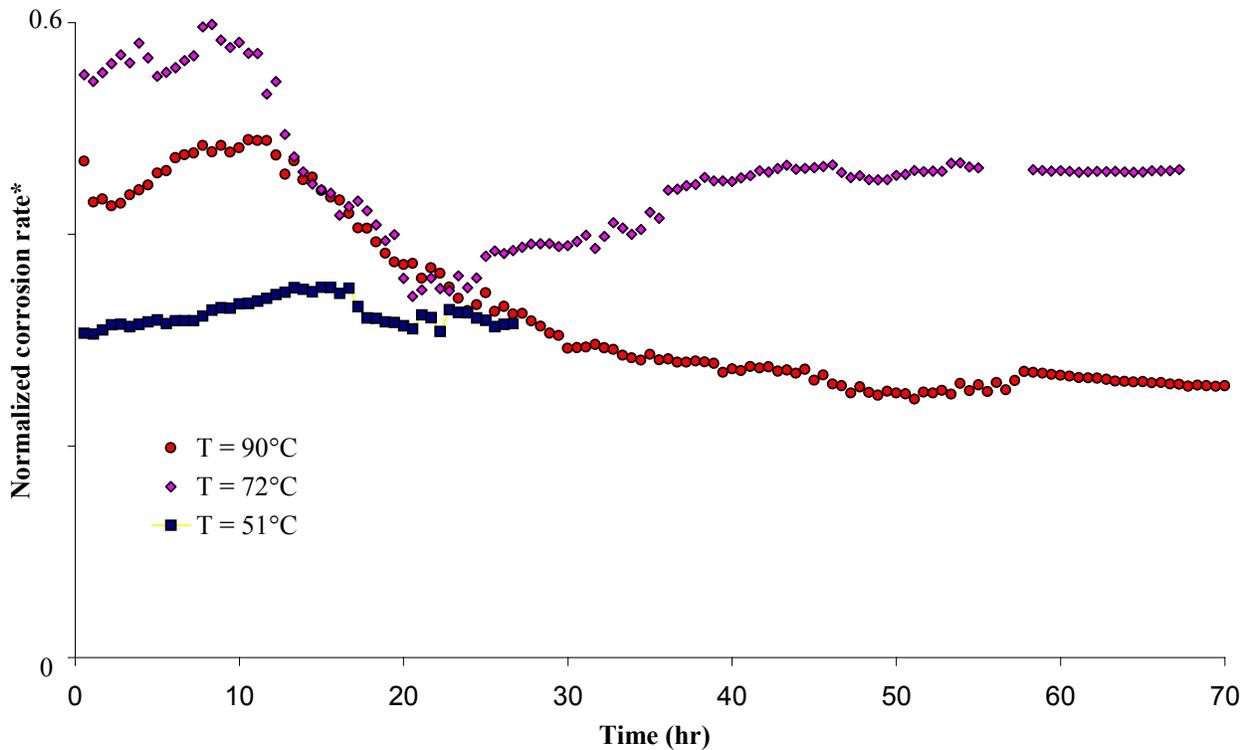
FIGURE 6: Corrosion rate vs time on E.R probe (Cormon). Influence of gas temperature.
$P_{CO2} = 4$ bar, $V_{gas} = 8$ m/s. High cooling.
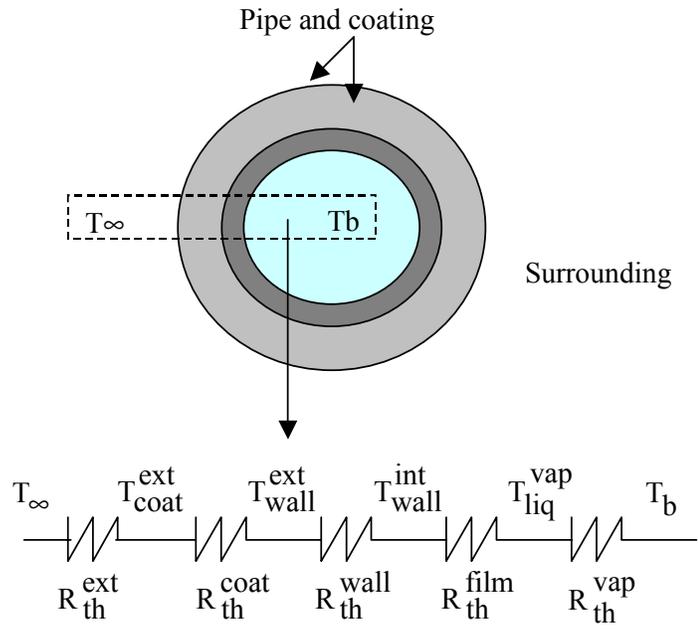
FIGURE 7: Equivalent circuit of heat transfer resistances for a pipeline and its surrounding
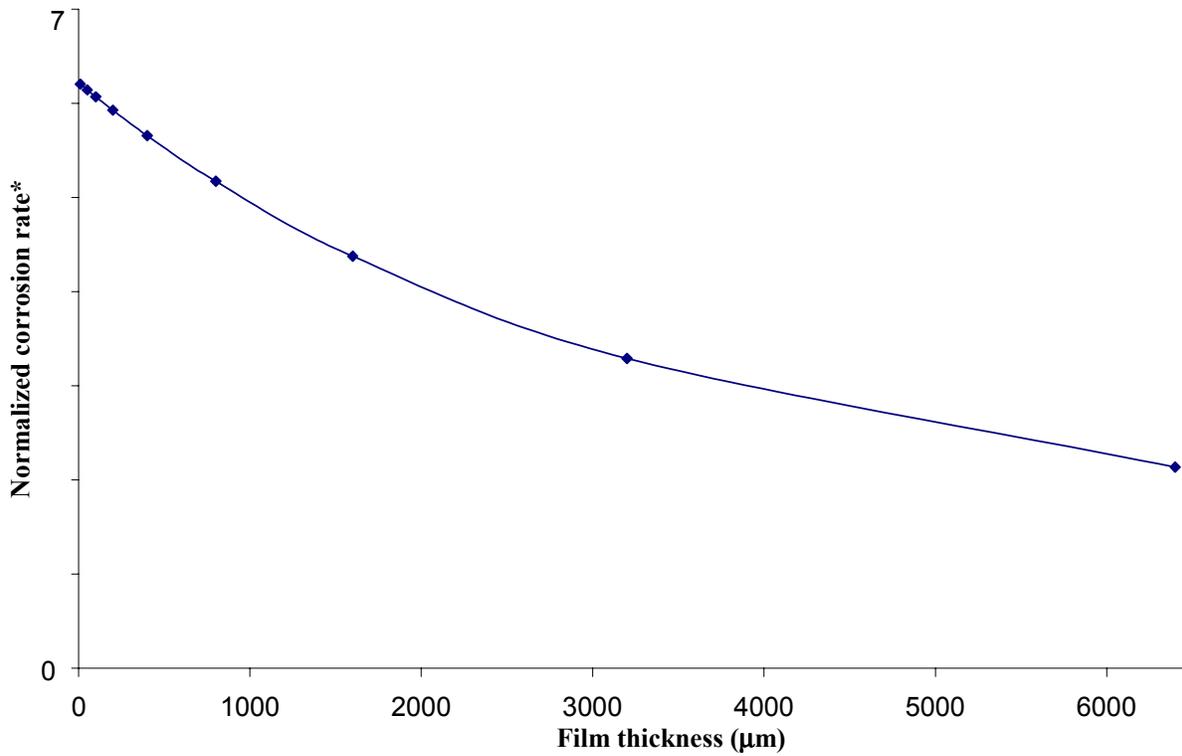
FIGURE 8: Simulated corrosion rate as a function of film thickness for stagnant condensed water (no convection). T =90°C, P_{CO2} = 4 bar
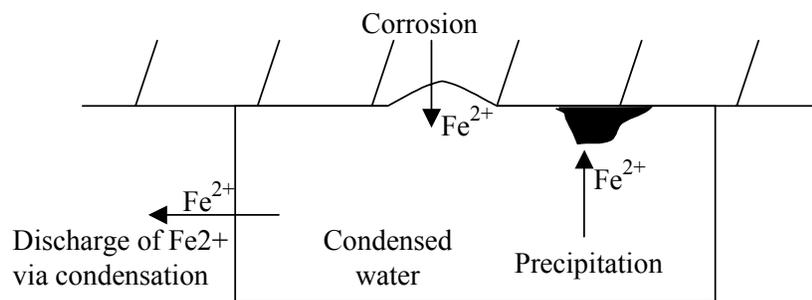
FIGURE 9: Transport, source, and sink of iron ions during TLC
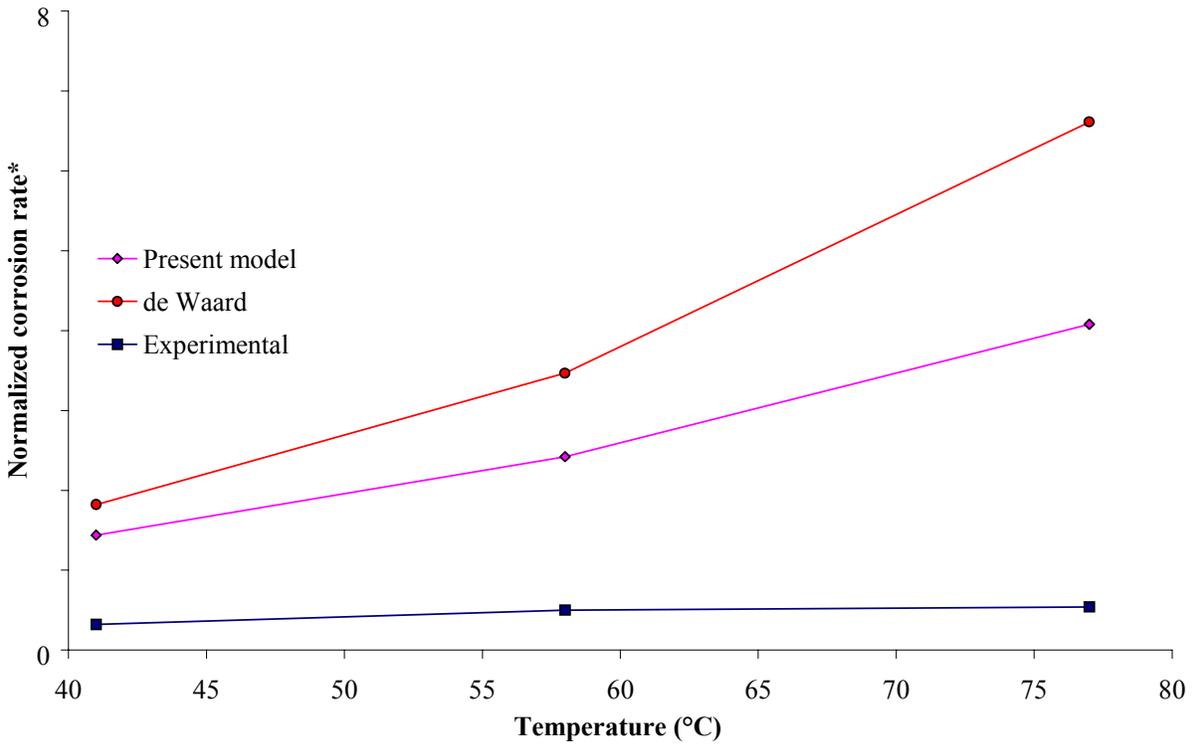
FIGURE 10: Comparison of the experimental and theoretical corrosion rates. Influence of temperature. P_{CO2} = 8 bar.
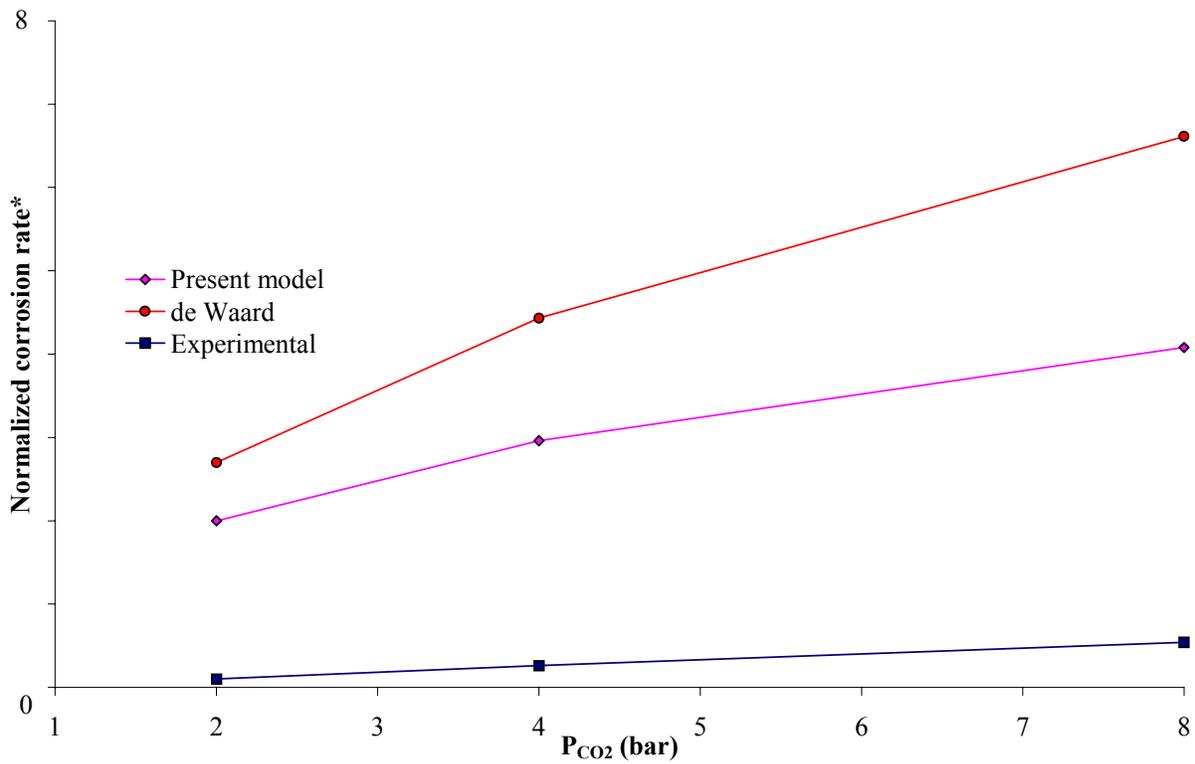
FIGURE 11: Comparison of the experimental and theoretical corrosion rates. Influence of the partial pressure of carbon dioxide. T_{gas} = 80°C
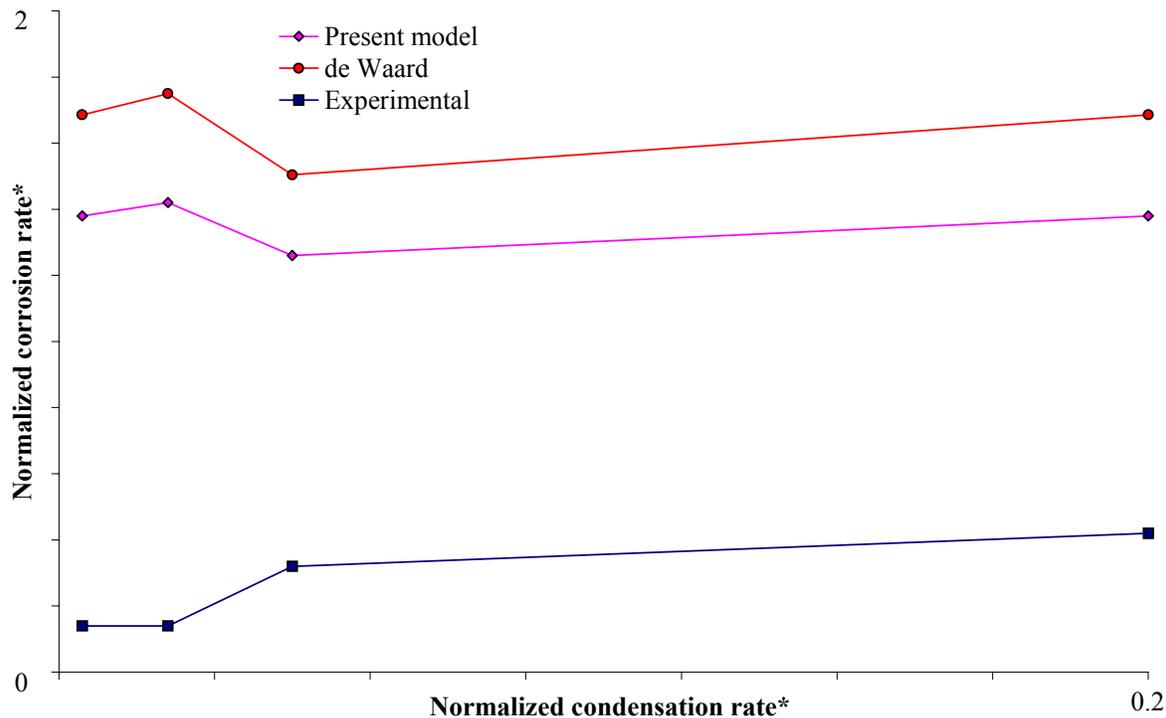
FIGURE 12: Comparison of the experimental and theoretical corrosion rates. Influence of the condensation rate. $T_{gas} = 50°C$, $P_{CO2} = 4$ bar
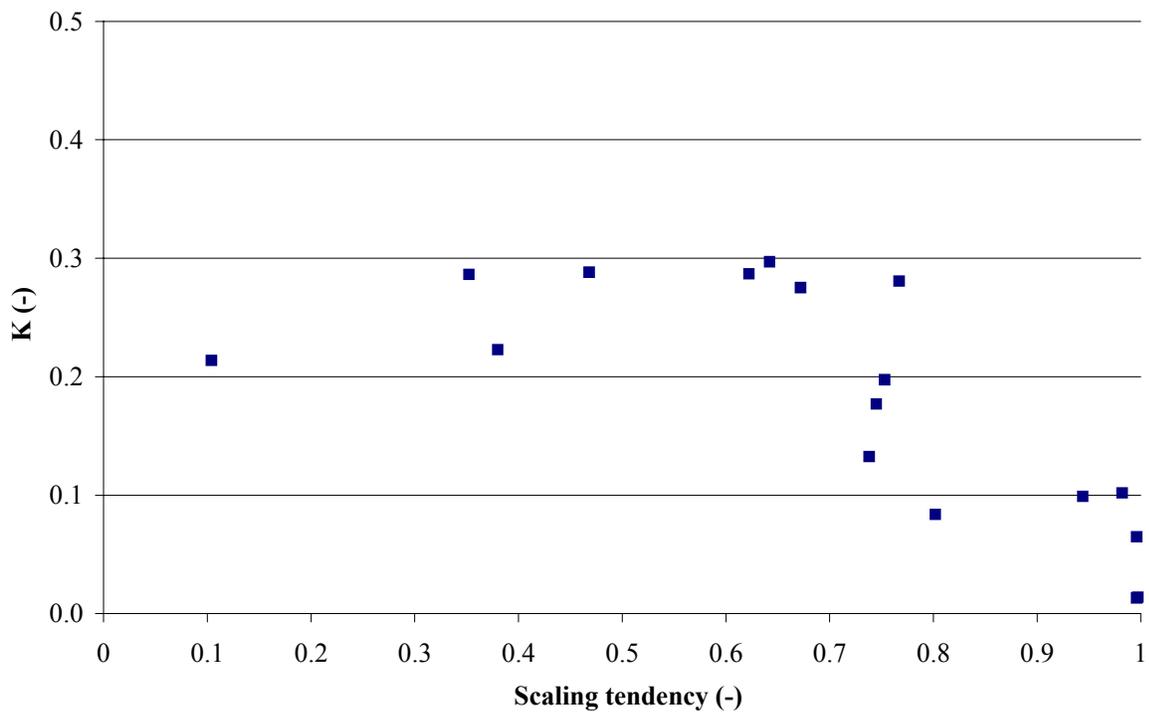
FIGURE 13: Factor K (1-K representing the surface coverage) as a function of the scaling tendency.